

Online Bearing Remaining Useful Life Prediction Based on a Novel Degradation Indicator and Convolutional Neural Networks

Cheng Cheng, Guijun Ma, Yong Zhang, Mingyang Sun, Fei Teng, Han Ding, and Ye Yuan

Abstract—In industrial applications, nearly half the failures of motors are caused by the degradation of rolling element bearings (REBs). Therefore, accurately estimating the remaining useful life (RUL) for REBs are of crucial importance to ensure the reliability and safety of mechanical systems. To tackle this challenge, model-based approaches are often limited by the complexity of mathematical modeling. Conventional data-driven approaches, on the other hand, require massive efforts to extract the degradation features and construct health index. In this paper, a novel online data-driven framework is proposed to exploit the adoption of deep convolutional neural networks (CNN) in predicting the RUL of bearings. More concretely, the raw vibrations of training bearings are first processed using the Hilbert-Huang transform (HHT) and a novel nonlinear degradation indicator is constructed as the label for learning. The CNN is then employed to identify the hidden pattern between the extracted degradation indicator and the vibration of training bearings, which makes it possible to estimate the degradation of the test bearings automatically. Finally, testing bearings’ RULs are predicted through using a ϵ -support vector regression model. The superior performance of the proposed RUL estimation framework, compared with the state-of-the-art approaches, is demonstrated through the experimental results. The generality of the proposed CNN model is also validated by transferring to bearings undergoing different operating conditions.

Index Terms—Remaining useful life estimation, rolling bearings, Hilbert-Huang transform, convolutional neural networks.

NOMENCLATURE

RUL	Remaining useful life.
DEI	Degradation energy indicator.
CNN	Convolutional neural network.
SVR	Support vector regression.
REB	Rolling element bearing.
HHT	Hilbert-huang transform.
EMD	Empirical mode decomposition.
IMF	Intrinsic mode function.

This work was supported by the National Natural Science Foundation of China under Grant 91748112 and by the Primary Research & Development Plan of Jiangsu Province [grant number BE2017002]. (Corresponding author: Prof. Ye Yuan)

Cheng Cheng and Ye Yuan are with School of Automation, State Key Lab of Digital Manufacturing Equipment and Technology, Huazhong University of Science and Technology, Wuhan, China, 430074.

Guojun Ma and Han Ding are with State Key Lab of Digital Manufacturing Equipment and Technology, Huazhong University of Science and Technology, Wuhan, China, 430074.

Yong Zhang is with School of Information Science and Engineering, Wuhan University of Science and Technology, Wuhan 430081, China.

Mingyang Sun and Fei Teng are with the Department of Electrical & Electronic Engineering, Imperial College London, London, SW7 2AZ, UK.

ETA	Exponential transformed accuracy.
MSE	Mean square error.
FT or L_{ft}	Failure threshold.
N	Length of historical units of training bearing.
Q	Length of historical units of test bearing.
U	No. of predicted units of test bearing.
S_i	Sensor measurement signal of i -th unit.
t_i	i -th recording phase.
τ	Time interval between two recording phases.
L	DEI of training bearing.
L_{norm}	Normalized DEI of training bearing.
L_{test}	Estimated DEI of test bearing.
$\hat{L}_{U,test}$	Predicted DEI of test bearing.
k	No. of convolutional layer.
W^k	Weights in k -th convolutional layer.
B^k	Bias in k -th convolutional layer.
$\hat{T}_{failure}$	Predicted RUL of test bearing.
$T_{failure}$	Real RUL of test bearing.
$E_r\%$	Relative percentage error of prediction.
X	Training set for SVR.
\mathbb{R}	The set of real numbers.
\mathbb{Z}	The set of positive integers.

I. INTRODUCTION

TO constrain relative motion while reducing friction between moving parts, rolling element bearings (REBs) are one of the most widely used elements in industrial machinery. Thus, prognostics and health management (PHM) of bearings is of significance for safety, reliability and effectiveness of the mechanical systems [1], [2], [3]. The literature show nearly half of motor failures are related to the degradation of bearings [4]. As such, estimating the remaining useful life (RUL) (i.e., time-to-failure prognostics) of bearings in maintenance strategies has attracted a great deal of attention in recent years [5]. RUL prediction helps users monitor the condition of the bearings and provides an estimation of time left before a failure occurs [6]. Compared with fault diagnosis, which has been well investigated over the past decades [7], the problem of RUL prediction studied this paper is a relatively new and challenging topic due to the huge amount of uncertainty of environment and operating condition [8].

In general, RUL prediction approaches can be categorized into two categories: model-based and data-driven approaches. The aim of model-based approach is to build a physical model to represent the degradation process of the rolling bearing

[9]. Li *et al.* [10] predicted the rate of defect growth on a bearing unit through using Paris's law for fatigue. However, it is difficult to construct a precise physical degradation model due to the sensitivity of the model parameters and noised operating environments. This limits the practical applications of the model-based approach. The data-driven approach investigated in this paper benefits from the extensive expertise in signal processing and machine learning [11], and infers the degradation process of bearings without knowing any of the physics of degradation failure. In the data-driven approach, the prognostic framework mainly consists of three stages: 1) feature extraction from the noisy bearing signals helps build up the useful information, such as health indicator, for learning of degradation behavior; 2) degradation models are trained on the training sets using statistical and machine learning techniques; and 3) the degradation indicator of the test bearings can be predicted based on the model trained in the last stage and the unknown degradation process can be predicted by applying regression techniques, such as ϵ -SVR.

To extract features from raw signals, time-domain, frequency-domain, and time-frequency domain analysis are commonly adopted. For analyzing non-stationary signals, such as the vibrations of REBs, time-frequency analysis has been found to be the most efficient technique due to its ability to characterize transient signals over time and frequency domains simultaneously [12]. The well-known time-frequency distributions for extracting bearing features include short-time Fourier transform [13], wavelets [14], Wigner-Ville distribution [15], and Hilbert-Huang transform (HHT) [16]. The short-time Fourier transform is limited by its time-frequency resolution capability; for instant, the low frequencies are difficult to identify with short windows. Wavelets and the Wigner-Ville distribution provide a richer picture than short-time Fourier transform; however, their effectiveness depends on estimating the Hurst parameter and the quality of the analyzed signal, respectively. In [17] and [18], HHT shows better computational efficiency and resolution over other time-frequency analyses. The HHT uses the techniques of empirical mode decomposition (EMD) and Hilbert transform (HT) to decompose the original vibration signal into a number of intrinsic mode functions (IMFs) in various frequency scales. In each IMF, the frequency components are related to both the sampling frequency and the signal itself, thus demonstrating that HHT is a self-adaptive signal processing technique perfectly suited to non-stationary signals. Wu *et al.* [19] analyze the time-to-failure prognostics of REBs, which extracts ten statistical features using time and frequency analysis and eleven IMF features using HHT time-frequency analysis. The gear fault identification method proposed in Cheng *et al.* [20] is based on the HHT and the first six IMFs are selected as inputs for SOM neural networks for fault diagnosis. Due to the power of deep-learning methods in feature detection, this paper simply extracts one time-series health indicator using HHT method, namely degradation energy indicator (DEI), as the label for the purpose of model training.

For RUL prediction, in the literature, existing techniques are mainly based on statistical and machine learning, such as artificial neural networks (ANN) [21], fuzzy logic systems

[22], auto-regressive (AR) models [8], and wiener process models [23]. The computational cost of ANN is relatively high in terms of optimizing the weights of the model [24]. The performance of the AR models and fuzzy logic systems require precise trend of historical observations and high-quality training data, respectively. Recently, deep learning has merged into research and industry fields, and has beaten other machine learning techniques in speech recognition [25] and image recognition [26], and many other domains. Deep learning architecture is composed of multiple layers in order to discover high level abstractions from labeled data using a back-propagation algorithm. The key aspect is that deep learning does not require human efforts to design the features on layers; they automatically learn feature representations. Recurrent neural network (RNN) for RUL is investigated in recent years [27]. It is inadequate to extract time-related features of signals acquired using high sampling frequencies, such as machinery vibrations or speech signals, some works using long short-term memory units (LSTMs) and gated recurrent units (GRUs) to get rid of this issue [28]. In contrast, as one of the most-known models in deep learning, CNN dominates in the field of computer vision for the recognition and detection problems.

1-D CNN, also named as time-delay neural net, has been applied with great success to speech recognition and document reading tasks [29]. These successes lay a solid foundation for the application of 1-D CNN in machinery system. In terms of this work, the main reason of applying CNN for RUL estimation is that the degradation feature shows local connection property. Previous experience proves that there are three states across bearing lifetime, namely good state, medium state, and degraded state. Vibration values within each state are highly correlated, demonstrating the local features are easily detected by CNN. In addition, bearing vibrations compose of non-stationary and stationary components and can be decomposed into fast to low oscillations. Thus, CNN will be success for our problem based on the fact that the bearing vibrations are compositional hierarchies. Hereby, this paper is the first paper (to our knowledge) exploiting the adoption of CNN in estimating the RUL of bearings, as a prognosis problem, to learn about degradation behavior according to raw vibration data and an extracted label by using the HHT.

In this work, we propose a new data-driven framework for predicting the RUL of REBs by applying the HHT, CNN, and ϵ -Support vector regressorion (ϵ -SVR). In the first step, the raw vibration signals collected from sensors are processed by the HHT method and a novel time-series degradation indicator, i.e., DEI, is constructed. Subsequently, a CNN model is trained to learn the features from the input raw vibration to the DEI label on the training bearings, and used to predict the DEIs of testing bearings. Then, a ϵ -SVR model is introduced so that the evolution of the degradation can be forecast till the bearing failure. The effectiveness of the proposed based framework for RUL prediction is validated on an experimental platform (i.e., PRONOSTIA). This work makes the following contributions:

- 1) In contrast to the problem with predicting the RUL stated in existing approaches, where a linear time degradation indicator normally is featured as the label for network

training [30], the proposed method successfully extracts a novel nonlinear degradation energy index (DEI) to describe the degradation trend of the training bearing, according to the nature frequencies of bearing components. The comparison of the time degradation indicator and the DEI is shown in Figure 1. It is observed that the nonlinear DEI experience a long time flat curve before a sharp degradation trend when it closes the end of bearing lifetime, which is close to the real degradation process of most machinery systems [31]. With the aggregation of damages at different bearing components close to the end of lifetime, the simple time degradation indicator is less effective and less robust than DEI for RUL estimation.

- 2) A novel CNN architecture is trained to reveal its hidden dependencies between the vibration data and the DEI of the training bearing. Instead of spending high computational power on extracting new health indicators for each individual testing bearing, the proposed CNN model could estimate the DEI automatically in a very short time ($\sim 10^{-4}$ s). The proposed CNN architecture is general and robust, it can transfer to another bearing undergoing different operating condition and obtain good prediction results, without changing CNN hyper parameters and the depth of layers. DEI, as the output of the CNN model of a test bearing, describes the degradation percentage of bearing's lifetime.
- 3) In this work, the maximum degradation value (i.e., failure threshold (FT)) is set as the maximum value of DEI for the training bearing after normalization. In this way, when estimating the RUL of a new bearing, the FT does not require to be pre-defined artificially which is extremely difficult as the FT has a large variation range between different bearings.
- 4) Much lower RUL prediction errors are achieved, compared with those of state-of-the-art approaches and the other tested methods in this paper, indicating the superior performance of the proposed method.

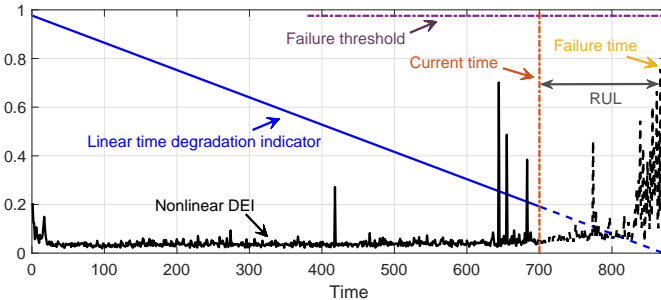


Figure 1. Linear time degradation indicator (blue) vs. nonlinear DEI (black), as a label for network training.

The outline of this paper is as follow. Section II presents the proposed RUL prediction framework and technical details. In Section III, the experimental results obtained from bearing degradation tests based on an experiment platform are provided. Thereby, the performance of the proposed framework is

validated and the results show improved accuracy in predicting the RUL compared with state-of-the-art approaches. Section IV summarizes the paper and discusses future works.

II. DATA-DRIVEN REMAINING USEFUL TIME ESTIMATION

To solve the above-stated problem in Section I, the overall framework for the prediction of the RUL can be decomposed into three parts. The schematic of the overall framework is shown in Fig. 2. The key challenges of this work involve: obtain the DEI to represent the degradation behaviour; establish a CNN model to map raw vibration signal to the DEI; and construct an ϵ -SVR to predict the RUL. Thus, in the following subsections, the explicit expression of degradation feature extraction, CNN model, and ϵ -SVR forecasting model will be derived in Section II-A, Section II-B, and Section II-C.

A. Degradation indicator extraction

To begin with, for a training bearing, it is assumed that the raw vibration signal till the end of lifetime with $N \in \mathbb{Z}$ historical units have been acquired. For the i th unit, the vibration signal is evenly measured at recording phase t_i , where $t_i = [t_{i1}, \dots, t_{ip}]$ and p is the number of measurements recorded in one unit, and the sensory measurement signal is denoted as $\mathbf{S}_i = [S_i(t_{i1}), \dots, S_i(t_{ip})] \in \mathbb{R}^{1 \times p}$ for $i \in D = \{1, 2, \dots, N\}$. These units can be used to extract the DEI sequence, denoted as $\mathbf{L} = [L_1, \dots, L_N] \in \mathbb{R}^{1 \times N}$.

EMD is a self-adaptive method which is normally applied to analyze non-stationary and nonlinear signals. It decomposes the raw vibration data, \mathbf{S}_i , into a number of IMFs, illustrating the natural oscillation modes from fast to low oscillations. A sifting process is adopted to calculate the j -th mode of IMF ($\text{IMF}_{i,j}$) of the i -th unit, using the following formula:

$$a_{i,j}^v(t_i) = a_{i,j}^{v-1}(t_i) - \omega_{i,j}^{v-1}(t_i), \quad j = 1, \dots, n \text{ and } v = 1, \dots, (1)$$

and

$$a_{i,j}^0(t_i) = \mathbf{S}_i(t_i) - \sum_{j=1}^{n-1} \text{IMF}_{i,j}, \quad j = 2, \dots, n \text{ and } a_{i,1}^0 = \mathbf{S}_i, \quad (2)$$

where $\omega_{i,j}^{v-1}(t_i)$ is the mean value of the upper bound and lower bound of process component $a_{i,j}^{v-1}(t_i)$. It repeats V times until $a_{i,j}^v(t_i)$ meets the following two conditions:

- (1) $a_{i,j}^v(t_i)$ should have one or zero difference between the extrema number and the number of zero crossing,
- (2) along the time axis, the average value of upper and lower bound of $a_{i,j}^v(t_i)$ should be zero everywhere,

then $\text{IMF}_{i,j} = a_{i,j}^v(t_i)$.

Once having the $\text{IMF}_{i,j}$ of \mathbf{S}_i , the analytical form of the $\text{IMF}_{i,j}$ can be written as:

$$\text{IMF}_{i,j}^A = \text{IMF}_{i,j} + i \text{IMF}_{i,j}^H. \quad (3)$$

$\text{IMF}_{i,j}^H$ is the Hilbert transformation of $\text{IMF}_{i,j}$ by convolution with function $\frac{1}{\pi t}$, given as:

$$\text{IMF}_{i,j}^H = \frac{1}{\pi} \int_{-\infty}^{+\infty} \frac{\text{IMF}_{i,j}(s)}{t-s} ds. \quad (4)$$

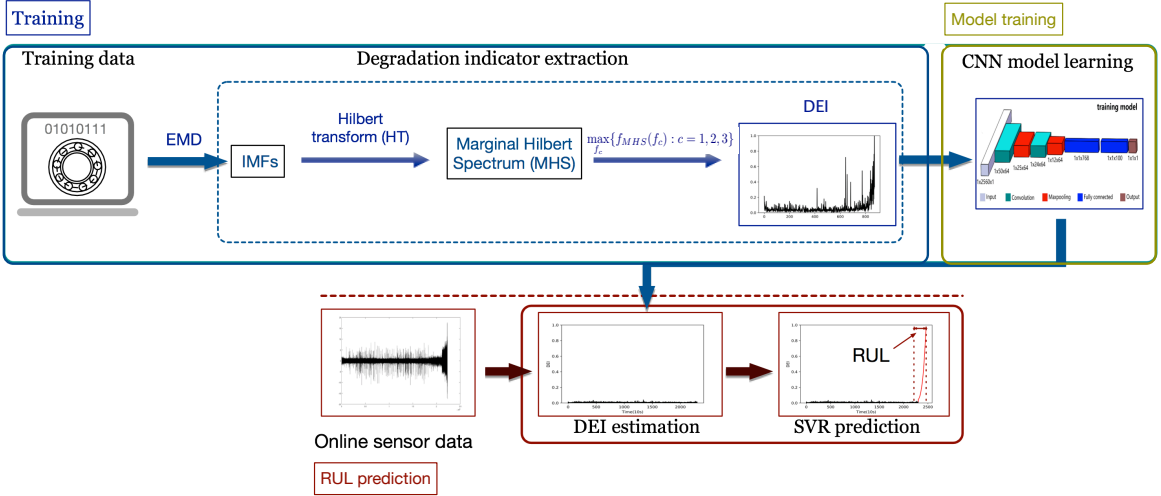


Figure 2. On-line data-driven RUL prediction framework. This framework involves three stages: (1) Training stage aims to extract the degradation indicator. The DEI is extracted using EMD, HT and marginal Hilbert spectrum (MHS), and the value of DEI is also related to the nature frequencies of different bearing components (f_c) for $c=1,2,3$; 2) Model training stage aims to train a CNN model based on the training data that discovers the hidden pattern for the DEI from the raw vibration data; and (3) On-line prediction stage predicts the RUL according to the trained CNN model and a ϵ -SVR forecasting model.

By this means, we can calculate the instantaneous amplitude $h_{i,j}(t_i)$ and phase $\phi_{i,j}(t_i)$, which are formulated as

$$\begin{aligned} h_{i,j}(t_i) &= \sqrt{(\text{IMF}_{i,j})^2 + (\text{IMF}_{i,j}^H)^2}, \\ \phi_{i,j}(t_i) &= \tan^{-1} \left(\frac{\text{IMF}_{i,j}^H}{\text{IMF}_{i,j}} \right). \end{aligned} \quad (5)$$

Thus, it is easy to derive the instantaneous frequency $f_{i,j}(t_i)$

$$f_{i,j}(t_i) = \frac{1}{2\pi} \frac{d\phi_{i,j}(t_i)}{dt}. \quad (6)$$

The Hilbert Spectrum of S_i is then given by

$$M_i(f_i, t_i) = \sum_{j=1}^n h_{i,j}(f_i, t_i). \quad (7)$$

The marginal Hilbert spectrum $M_i(f)$ can be written as:

$$M_i(f_i) = \int M_i(f_i, t_i) dt_i. \quad (8)$$

The nature frequencies of bearing components depend on the geometry of the bearing and its rotation speed, where the expression of these frequencies are given in Table I. In where η is the number of balls, f_ω is the rotation frequency, Φ is the contact angle, and ℓ_{ball} and ℓ_{pitch} are the ball diameter and pitch diameter, respectively.

Table I

BEARING FREQUENCIES OF INNER RACE, OUTER RACE AND BALL[32]

Symbol	Description	Expression
f_{inner}	Inner race frequency	$\frac{\eta}{2} \cdot f_\omega \cdot \left(1 + \frac{\ell_{ball}}{\ell_{pitch}} \cdot \cos \Phi \right)$
f_{outer}	Outer race frequency	$\frac{\eta}{2} \cdot f_\omega \cdot \left(1 - \frac{\ell_{ball}}{\ell_{pitch}} \cdot \cos \Phi \right)$
f_{ball}	Ball frequency	$\frac{\ell_{ball}}{\ell_{pitch}} \cdot f_\omega \cdot \left(1 - \frac{\ell_{ball}^2}{\ell_{pitch}^2} \cdot \cos^2 \Phi \right)$

With the bearing frequencies of different components, the degradation index DEI L is defined as the maximum value of the MHS by substituting the f_{inner} , f_{outer} and f_{ball} in Eq. (9), given as:

$$L_i = \max [M_i(f_{inner}, f_{outer}, f_{ball})], \quad i \in D. \quad (9)$$

B. Modelling for degradation indicator estimation

In this work, a series of layers with repeated components are stacked in the CNN architecture, including convolutional layer, pooling layer, fully connected layer and regression layer [33].

Convolution layer contains organized patches in convolutional layers, each patch is calculated by composing the features of the previous layer through a filter bank with the following equation:

$$u_m^k = W^k * u_e^{k-1} + B^k, \quad (10)$$

where $u_m^k \in \mathbb{R}$ denotes the output of the m -th unit in the k -th layer. $u_e^{(k-1)} \in \mathbb{R}^{1 \times o^k}$ is the input data the e -th sub-vector in the previous layer $k-1$, where o^k is kernel size in layer k . $W^k \in \mathbb{R}^{1 \times o^k}$ and $B^k \in \mathbb{R}$ denote the connecting weights and bias in the k -th layer, respectively. '*' means the convolution operation. It is noted that when $k=1$, $u_e^{(k-1)}$ is a sub-vector of the raw vibration data S_i . Here we define all neurons in each layer is $u^k = [u_1^k, \dots, u_m^k, \dots, u_{G_k}^k]$ for $k \in D_k = \{1, 2, \dots, K\}$, where $G_k \in \mathbb{Z}$ is the number of neurons in k -th layer. For convolutional layer, $G^k = (G^{k-1} - o^k) / I_{cv}^k + 1$ and $I_{cv}^k \in \mathbb{Z}$ is the stride in convolutional layer.

Activation function is introduced after convolution layer. Among various activation functions, Rectified linear unit (ReLU) $r_m^k = \max(0, u_m^k)$ is chosen as the nonlinear activation function to prevent the issue of vanishing gradient which may significantly increase the training time or even lead to the non-convergence.

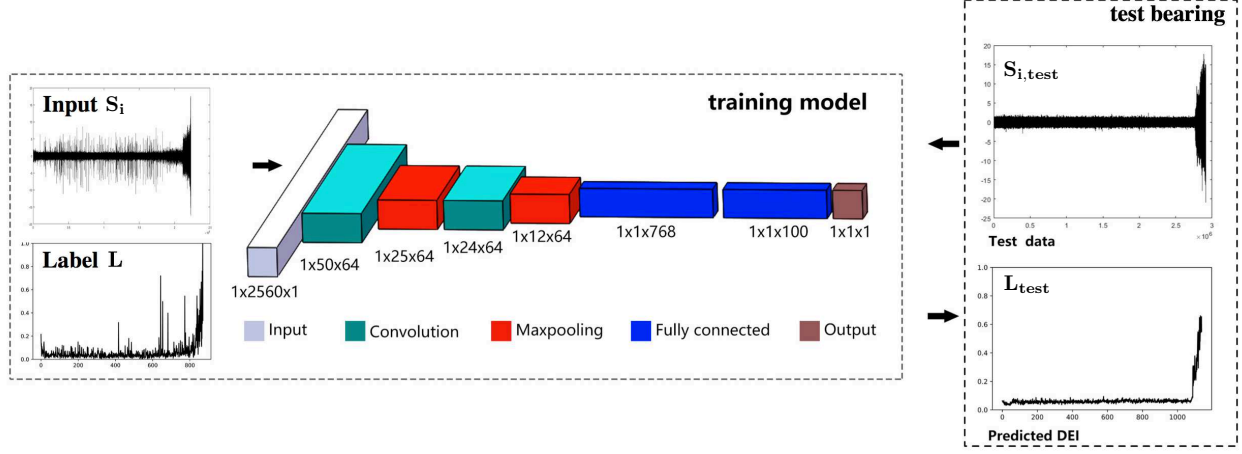


Figure 3. The CNN architecture of this work. Normalized DEI \mathbf{L} is used as the label for training. A 5-layer CNN model is trained to map the raw vibration data \mathbf{S}_i (input) to the DEI \mathbf{L} (output). For a new test bearing, the vibration data $\mathbf{S}_{i,test}$ is then directly input to the proposed CNN model to obtain the estimated DEI \mathbf{L}_{test} .

Pooling layer is then used as a nonlinear down-sampling layer extracts the maximum feature values in each patches of the input data. Its function is to save computation time and downsize the number of parameters of the model as well as control overfitting. More specifically, pooling transforms small windows into single values by maxing or averaging. Consequently, the features extracted within the small window are similar and therefore illustrating the main property of CNN, the shift invariance. Compared with average-pooling, max-pooling has been demonstrated with better performance in the literature [34], which is given by:

$$P_m^k = \max_{\gamma=1, \dots, \lambda^k} r_{\gamma+(m-1)I_{pl}^k}^{(k-1)}, \quad (11)$$

where $\lambda^k \in \mathbb{Z}$ is the pooling size, and I_{pl}^k is the stride in max pooling.

Regression layer is the last layer of our proposed CNN architecture. Since we use a normalized DEI \mathbf{L} as the label for learning, the sigmoid function $\text{sigm}(\mathbf{u}^{K-1})$ with an output value between (0,1) is applied to the last layer for normalized output. In the last layer, it is obvious that $N = G^K$. Hereby, mean square error (MSE) function is used to compute the loss with the expression:

$$z = \frac{1}{N} \sum_{m=1}^N (L_m - \tilde{L}_m)^2, \quad (12)$$

in where the proposed CNN model is minimizing the loss function z between ground label DEI \mathbf{L} and predicted label $\tilde{\mathbf{L}}$. To summarize, the proposed CNN modeling is outlined in Algorithm 1.

With the obtained CNN model, for a new test bearing with $Q \in \mathbb{Z}$ historical units, the estimated DEI $\mathbf{L}_{test} = [L_{1,test}, \dots, L_{Q,test}] \in \mathbb{R}^{1 \times Q}$ can be automatically generated by the trained CNN with the new vibration signal \mathbf{S}_i , where $i \in D_{test} = \{1, \dots, Q\}$.

Algorithm 1 Outline of CNN training for DEI estimation

Input : The extracted DEI label \mathbf{L} ;
 The raw vibration data \mathbf{S}_i .
Output: Trained CNN parameters: W^k and B^k
 Initialize parameters;
repeat
Forward Propagation:
do
 Conducting convolution operation with the raw vibration data using Eq. (10).
 Use ReLU as the nonlinear activation function.
 Max-pooling function Eq. (11) is employed to extract the maximum feature values.
end;
 Conventional fully-connected layer is used for DEI regression.
 The sigmoid function is introduced for normalized output.
 Compute the MSE with the loss function Eq. (12).
Backward Propagation:
 Compute the gradient using Adam [35] and update network parameters W^k and B^k .
until Maximum iterations;
 Use the trained CNN to estimate the DEI \mathbf{L}_{test} on the test bearing.

C. Prognostic

Then, to predict the RUL $\hat{T}_{failure} \in \mathbb{R}$, a ϵ -SVR forecasting [36] model is formalized to predict the upcoming degradation $\hat{L}_{Q+1,test}, \hat{L}_{Q+2,test}, \dots$ based on the estimated DEI \mathbf{L}_{test} by sliding window method. The forecasting process can be briefly categorized into 3 sub-steps:

- 1) Extract training features from the estimated DEI \mathbf{L}_{test} over a sliding window. The schematic of this step is illustrated in Fig. 4. The estimated DEI \mathbf{L}_{test} is decomposed into overlapping windows associated

with sampling window size l and sliding size s . $x_g = (\mu_g, \sigma_g^2)$ for $g \in \{1, \dots, \frac{Q-l-1}{s} + 1\}$ represents a training feature for ϵ -SVR, where μ denotes the mean value and σ^2 denotes the variance of each sampling window l . Thus, the training set for ϵ -SVR $\mathbf{X} = [(x_1, L_{l+1,test}), \dots, (x_g, L_{(g-1)s+l+1,test}), \dots, (x_{\frac{Q-l-1}{s}+1}, L_{Q,test})]$ is obtained, where $L_{(g-1)s+l+1,test}$ corresponds to the next value in \mathbf{L}_{test} of g -th sampling window;

- 2) ϵ -SVR modelling is described in Algorithm 2, while at the application level, two parameters (distance limit $\epsilon \in \mathbb{R}$ and penalty parameter $C \in \mathbb{R}$) can be set manually when training the prediction model. A radial basis function (RBF) is necessary when we intends to train a nonlinear model;
- 3) The SVR model $f(x)$ learned in Algorithm 2 is then used to predict the RUL by sliding window method (with the same l and s in step 1). Since the test bearing undergoing same operating condition as the training bearing, it is reasonable to define the FTs (denoted as L_{ft}) of the test bearing equals to the last feature of the DEI of the training bearing, such that $L_{ft} = L_N$. Hence, the first prediction can be calculated as $\hat{L}_{Q+1,test} = f(x_{\frac{Q-l}{s}+1})$, and the predicted DEI $\hat{\mathbf{L}}_{U,test} = [\hat{L}_{Q+1,test}, \dots, \hat{L}_{Q+U,test}]$ can be obtained by shifting the sampling window, with $\hat{L}_{Q+U-1,test} \leq L_{ft} \leq \hat{L}_{Q+U,test}$. This will consequently lead to $\hat{T}_{failure} = U \times \tau$, where τ is the time interval between two recording phases.

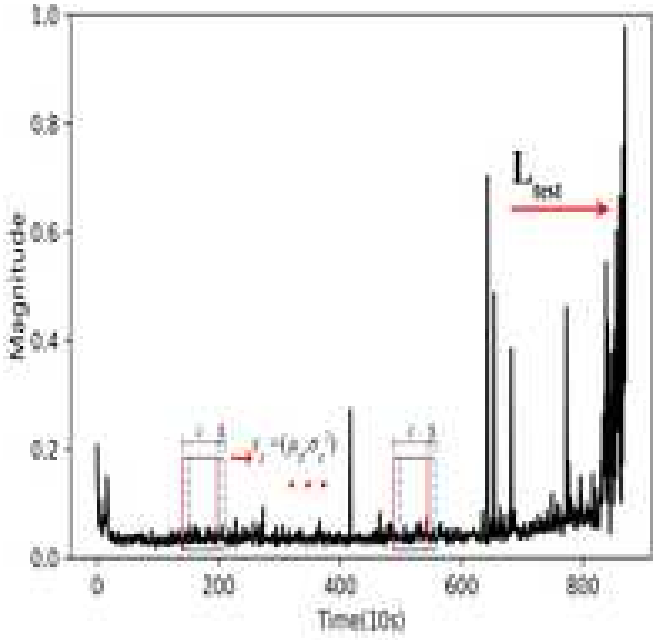


Figure 4. The diagram of extracting features for ϵ -SVR prediction, where l is the sampling window size, s is the sliding size, and x_g stores the mean value μ_g and variance σ_g^2 of each sampling window.

Algorithm 2 Framework of ϵ -SVR.

Require:

A training set \mathbf{X} ;

A distance limit ϵ and a penalty parameter C ;

A kernel function named RBF with the equation: $\kappa(x_g, x_q) = \exp(-\frac{\|x_g - x_q\|^2}{2\sigma^2})$, σ is the width of RBF and $\sigma > 0$;

Ensure:

A regression model like $f(x) = w^\top \phi(x) + b$, where w and b are optimized parameters and $\phi(x)$ is the x -mapped eigenvector that satisfies the equation: $\kappa(x_g, x_q) = \langle \phi(x_g), \phi(x_q) \rangle$.

Step 1: Establish optimization problems using C , ϵ , \mathbf{X} , and two slack variables ξ_g and $\hat{\xi}_g$ (slack degree for upper boundary and lower boundary, respectively) as following:

$$\begin{aligned} & \min_{w, b, \xi_g, \hat{\xi}_g} \frac{1}{2} \|w\|^2 + C \sum_{g=1}^{\frac{Q-l-1}{s}+1} (\xi_g + \hat{\xi}_g) \\ & \text{s.t. } f(\phi(x_g)) - L_{(g-1)s+l+1,test} \leq \epsilon + \xi_g, \\ & \quad L_{(g-1)s+l+1,test} - f(\phi(x_g)) \leq \epsilon + \hat{\xi}_g, \\ & \quad \xi_g \geq 0, \hat{\xi}_g \geq 0. \end{aligned}$$

Step 2: Add Lagrangian multipliers for each constraint: $\mu_g \geq 0, \hat{\mu}_g \geq 0, \alpha_g \geq 0, \hat{\alpha}_g \geq 0$ and get the Lagrange function of formula 1:

$$\begin{aligned} L(w, b, \alpha, \hat{\alpha}, \xi, \hat{\xi}, \mu, \hat{\mu}) &= \frac{1}{2} \|w\|^2 + C \sum_{g=1}^{\frac{Q-l-1}{s}+1} (\xi_g + \hat{\xi}_g) - \sum_{g=1}^{\frac{Q-l-1}{s}+1} \mu_g \xi_g - \sum_{g=1}^{\frac{Q-l-1}{s}+1} \hat{\mu}_g \hat{\xi}_g + \\ & \sum_{g=1}^{\frac{Q-l-1}{s}+1} \alpha_g (f(\phi(x_g)) - L_{(g-1)s+l+1,test} - \epsilon - \xi_g) \\ & + \sum_{g=1}^{\frac{Q-l-1}{s}+1} \hat{\alpha}_g (L_{(g-1)s+l+1,test} - f(\phi(x_g)) - \epsilon - \hat{\xi}_g). \end{aligned}$$

Step 3: Substitute $f(\mathbf{X})$ into the formula 2, we firstly compute the gradient of $L(w, b, \alpha, \hat{\alpha}, \xi, \hat{\xi}, \mu, \hat{\mu})$ with respect to w, b, ξ_g and $\hat{\xi}_g$ and make it equal to zero. Then get the following results:

$$\begin{aligned} w &= \sum_{g=1}^{\frac{Q-l-1}{s}+1} (\hat{\alpha}_g - \alpha_g) \phi(x_g), \quad 0 = \sum_{g=1}^{\frac{Q-l-1}{s}+1} (\hat{\alpha}_g - \alpha_g), \\ C &= \alpha_g + \mu_g, \quad C = \hat{\alpha}_g + \hat{\mu}_g. \end{aligned}$$

Step 4: Substitute formula 3 into formula 2, and get a dual problem:

$$\begin{aligned} & \max_{\alpha, \hat{\alpha}} \sum_{i=g}^{\frac{Q-l-1}{s}+1} L_{(g-1)s+l+1,test} (\hat{\alpha}_g - \alpha_g) - \epsilon (\hat{\alpha}_g + \alpha_g) \\ & \quad - \frac{1}{2} \sum_{g,q=1}^{\frac{Q-l-1}{s}+1} (\hat{\alpha}_g - \alpha_g) (\hat{\alpha}_q - \alpha_q) \phi(x_g)^\top \phi(x_q) \\ & \text{s.t. } \sum_{g=1}^{\frac{Q-l-1}{s}+1} (\hat{\alpha}_g - \alpha_g) = 0, \\ & \quad 0 \leq \alpha_g, \hat{\alpha}_g \leq C. \end{aligned}$$

Step 5: The above process meets Karush–Kuhn–Tucker (KKT) constraints, which means at least one of α_g and $\hat{\alpha}_g$ is equal to 0. A sequential minimal optimization algorithm is used to solve α_g or $\hat{\alpha}_g$. Parameter b is calculated by substituting the α_g to get the mean value. The final regression model is described as:

$$f(x) = \sum_{g=1}^{\frac{Q-l-1}{s}+1} (\hat{\alpha}_g - \alpha_g) \kappa(x, x_g) + b$$

III. EXPERIMENTS

A. Data description

The validation of the proposed RUL prediction framework is done on an experimentation platform (PRONOSTIA) (see Fig. 5). This platform is built as a combination of three parts: rotating, loading, and measurement. The rotation of the test bearing is driven by the low speed shaft whose rotating torque is transmitted from the AC motor. A radial force generated by the loading part is applied on the external ring of the test bearing. Since this external radial force exceed the bearing's allowable dynamic load, the degradation behavior is accelerated so that we can observe its degradation process within a relatively short time (few hours). The horizontal and vertical vibrations of the bearing is commonly used for fault and prognosis analysis. During the experiment tests, two high-frequency accelerometers (Type DYTRAN 3035B) are placed orthogonally on the external race of the test bearing to acquire the horizontal and vertical vibrations separately. In this work, we extract our degradation labels by using the horizontal vibrations of bearings.

Bearing1 on the platform is chosen to validate the proposed framework. More specifically, the training set bearing1_2 is used for extracting the DEI and training the CNN model. Test sets bearing1_4, bearing1_5, and bearing1_6 are then used for estimating their DEIs and predicting the RULs by applying ϵ -SVR forecasting model. Results of the Bearing2 under different rotational frequency and external dynamic load are also provided and compared. The geometry parameters and the operation conditions of the bearing1 and bearing2 used in this work are listed in Table II. 2560 measurements (p) are collected at a fixed time interval $\tau = 10s$ with a sampling frequency of 25.6kHz. More detailed description of the dataset, bearings, and sensors can refer to the data description in [37].

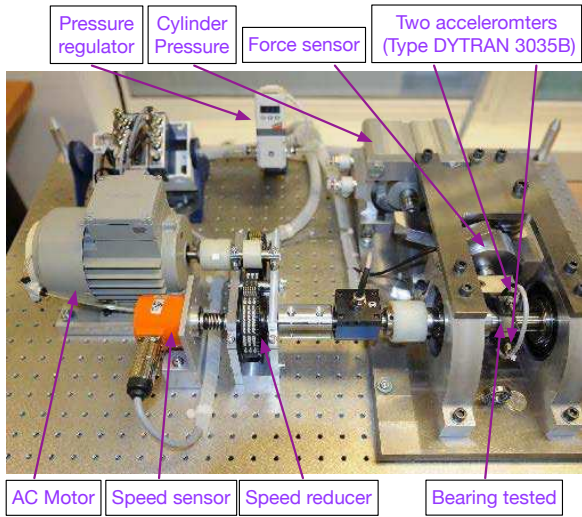


Figure 5. Overview of the PRONOSTIA platform [37].

B. Degradation indicator extraction

The DEI \mathbf{L} of the bearing1_2 is extracted from the MHS by substituting the outer ring frequency $f_{outer} = 168$ Hz, the inner ring frequency $f_{inner} = 221$ Hz, and the ball frequency $f_{ball} = 215.4$ Hz. into Eq. (9). The evolution of the extracted DEI of the bearing 1_2 is showed in Fig. 6(a).

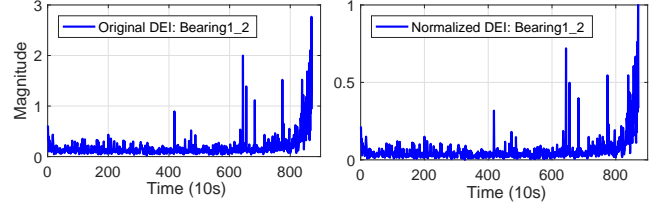


Figure 6. Evolutions of (a) original DEI and (b) normalized DEI.

C. Degradation indicator online estimation

The extracted DEI \mathbf{L} is used as the label for CNN, a normalization is necessary before training:

$$\mathbf{L}_{norm} = \frac{\mathbf{L} - \min(\mathbf{L}) \cdot \mathbf{1}_N}{\max(\mathbf{L}) \cdot \mathbf{1}_N - \min(\mathbf{L}) \cdot \mathbf{1}_N} \pm \epsilon, \epsilon \rightarrow 0 \quad (13)$$

where symbol $\mathbf{1}_N := [1, 1, \dots, 1]_{1 \times N}$.

According to the characteristic of the Sigmoid function, ϵ is an infinitesimal that used to avoid the value of label equal to 0 or 1. The normalized DEI is shown in Fig. 6(b). We use the vibration signal in the horizontal direction of the bearing1_2 as the input of the CNN, and the normalized DEI is used as the label which contains historical units $N = 871$. As shown in Fig. 3, our CNN model consists of $k=5$ layers: two convolutional layers (Conv1 and Conv2), two max-pooling layers (Maxpooling1 and Maxpooling2), and one fully connected layer (FC1). Before model training, Adam is set to be the optimizer with a small value 0.00001. The activation function in output layer is defined as Sigmoid function, ReLU function is used in the previous layers. Details of parameters in the proposed CNN model are concluded in Table III. The convolutional window sizes (kernel sizes) of convolutional layers are set to a large value 100 and a small value 2, respectively. The kernel size of Conv1 is relevantly large in order to extract more features from the raw vibration signal for more impressive power, meanwhile, small kernel size is

Table II
PHYSICAL CHARACTERISTICS AND OPERATION CONDITION OF ROLLING BEARINGS

Physical parameter	Value
Number of balls of the bearing (η)	13
Ball diameter of the bearing (ℓ_{ball})	3.5 mm
Pitch diameter of the bearing (ℓ_{pitch})	25.6 mm
Contact angle of the bearing (Φ)	0°
Rotation frequency (f_ω), bearing1	1800 r/min
Rotation frequency (f_ω), bearing2	1600 r/min
Maximum dynamic load (F), bearing1	4000 N
Maximum dynamic load (F), bearing2	4200 N

selected for Conv2 to prevent overfitting. After 1000 iterations of training, we use the trained parameters to predict DEIs of the training bearing1_2 and other three test bearings which have the same working condition in the experiment platform.

The estimated DEIs \mathbf{L}_{test} as the output of the CNN model are shown in Fig. 7. In Fig. 7(a), estimated DEI of the training bearing1_2 shows the similar time evolution as the DEI label in Fig. 6(b). The final estimated DEI value of the bearing1_2, $L_{tf} = 0.9756$, is defined as the failure threshold for the test bearings in Fig. 7(b)-(d).

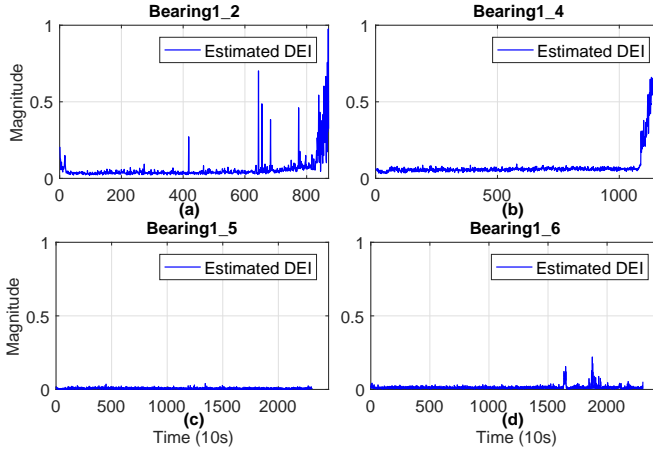


Figure 7. The estimated DEIs as the output of the proposed CNN model: (a) bearing1_2, (b) bearing1_4, (c) bearing1_5, and (d) bearing1_6.

D. Prognostic

As presented in Section III-C, the estimated DEIs have obtained from the trained CNN model. However, the DEIs of the test sets shown in Fig. 7(b)-(d) do not reach their fault limit, which need a regression prediction for the latter degradation. A ϵ -SVR method is proposed to predict the upcoming degradation process of the test bearings. We conduct a training on the predicted DEI of the bearing1_2. The sampling window size l and the moving size s in Fig. 4 is set to 50 and 1, respectively. The kernel function used in the prediction case is an RBF and penalty parameter C of the error term is chosen as 5.09. We estimate the DEI after 1000 steps based on the existing DEI, and using the maximum value of predicted DEI of bearing1_2 (i.e., $L_{tf} = 0.9756$) to limit the termination time of the test sets.

Table III
PARAMETERS IN THE CNN MODEL

Layer	Filters	Kernel size/Stride	Output size
Input	1x2560x1
Conv1	64	1x100/50	1x50x64
Maxpooling1	...	1x2/2	1x25x64
Conv2	64	1x2/1	1x24x64
Maxpooling2	...	1x2/2	1x12x64
Flatten	1x768
FC1	1x100
Output	1x1

Fig. 8(b)-(d) show the predicted RULs $\widehat{T}_{\text{failure}}$ of the test bearings till the failures occur. Red lines represent the predicted evolution of the bearings' degradation behavior using the ϵ -SVR method. The RULs are calculated as the difference between the final time when DEI reaching the failure threshold and the time of the last known point of the test bearings. For bearing1_4, the predicted RUL is 340s, while 1500s and 1480s are the predicted RULs for bearing1_5 and bearing1_6, respectively.

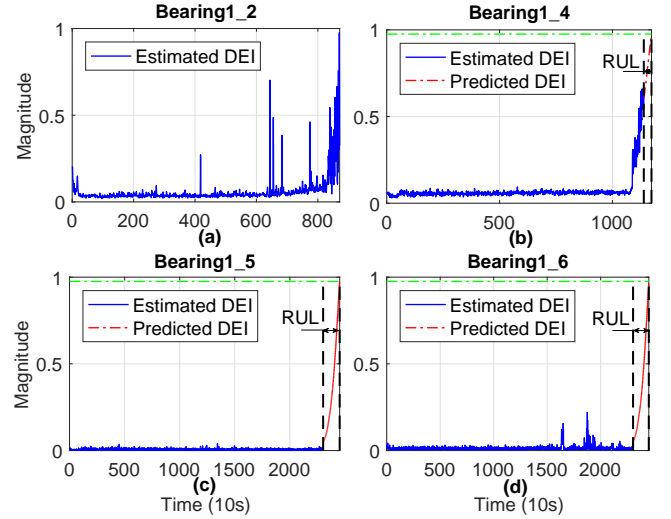


Figure 8. Plot (a) shows the estimated DEI of the bearing1_2. Predicted RULs of the test bearings are (b) 340 s for bearing1_4, (c) 1500 s for bearing1_5, and (d) 1480 s for bearing1_6. Green dotted lines in (b)-(d) represent the failure threshold.

E. Comparison

To assess the accuracy of the proposed method and compare to other existing approaches, two metrics are commonly adopted: 1) The relative percentage error ($Er\%$) which is given by Eq. (14); and 2) The exponential transformed accuracy (ETA) proposed in IEEE PHM 2012 [37]. ETA is an assessment index to distinguish the seriousness of the underestimate and overestimate of RUL prediction. It is clearly that underestimate (i.e., early warning) is preferred than overestimate (i.e., warning after damage) to prevent more severe damage of the bearing. The formulas are expressed in Eq. (15).

$$Er\% = 100\% \times \frac{T_{\text{failure}} - \widehat{T}_{\text{failure}}}{T_{\text{failure}}} \quad (14)$$

$$\text{ETA} = \begin{cases} \exp(-\ln(0.5)\frac{Er}{5}) & \text{if } Er \leq 0 \\ \exp(+\ln(0.5)\frac{Er}{20}) & \text{if } Er > 0 \end{cases} \quad (15)$$

where where T_{failure} is the real RUL for the test bearing. A higher $|Er\%|$ means a worse RUL prediction result. On the other hand, ETA value varies from 0 to 1, and a higher score means a better RUL prediction result. In this work, $Er\%$ is the common choice of most previous literature, thus it will be used for the comparison.

To verify the benefits of the DEI and CNN techniques on RUL prediction, here we also develop other two tested

methods for comparison purpose. The proposed method and the tested methods are denoted and explained as follows:

- 1) *C1: CNN and ϵ -SVR*: Without extracting the nonlinear DEI, this tested method uses a conventional linear time degradation label for CNN training. By this means, we can illustrate the impact of DEI on the prediction of the final RUL.
- 2) *C2: DEI and ϵ -SVR*: Without training the CNN model for feature extraction, DEI in this tested method is extracted manually and the ϵ -SVR is followed for RUL prediction. Note that computing a DEI for a new bearing requires high computational power and longer time. In the meantime, the FT of each test bearing has to be predefined artificially, which increase uncertainties of the RUL prediction affected by different working conditions. By this means, we can illustrate the impact of CNN modeling on the prediction of the final RUL.
- 3) *Proposed method: DEI based CNN and ϵ -SVR*: This is the proposed framework that on-line estimate the RUL for the REBs, integrating DEI extraction, CNN and ϵ -SVR into one framework.

Table IV summarizes the above methods.

Table IV
PROPOSED METHOD AND TESTED METHODS FOR COMPARISON

	DEI	CNN	SVR
<i>C1</i>	-	✓	✓
<i>C2</i>	✓	-	✓
<i>Proposed method</i>	✓	✓	✓

The predicted numerical errors of the test bearings with the proposed approach and the tested methods are listed in Table V. Our approach achieves $E_r\%$ of -0.29%, 7.45%, and -1.37% for bearing1_4, bearing1_5, and bearing1_6, respectively. It can be seen that the proposed approach achieves the smallest prediction errors comparing with the C1 and C2 methods. C1 uses a linear time degradation label for the training of the CNN model. The results show more than 19% prediction errors for test bearings and even 91.15% prediction error is obtained from bearing1_4, indicating that time degradation label is less effective than the DEI for the CNN training process. C2 is the method extracting the degradation indicator of the test bearings and define the FTs manually. As testing bearing1_4, 1_5, and 1_6 operate under same working conditions of bearing1_2, we employ the maximum and minimum value of bearing1_2 to normalize the extracted DEIs of C2 method. With same working condition and same normalization parameters, FT of the proposed method could reasonable be used in C2 as well. To evaluate the impact of CNN modeling on the estimation of the final RUL, for the test bearings, the estimated DEIs extracted using HHT and calculated by trained CNN model are compared in Figure 9. Without the CNN modeling procedure, one of the main drawback of the C2 method is that it requires long time to calculate (~ 2 s of each sampling period). This limits the practical application of this method in industry. Moreover, Figure 9(a) shows that due to the uncertainties and huge mount of noise, the DEI extracted by C2 method has

already exceeded the FT before the exact failure time, resulting in a 100% E_r . Similarly, in Figure 9(c), the DEI extracted of C2 method is much noised than it of proposed method. At 16470s, the magnitude of DEI:C2 is almost close to the FT, this phenomenon might lead to a waste of sources due to much underestimated of RUL. The comparison results in Table V demonstrate the benefits of using DEI and CNN in estimating the RUL of REBs.

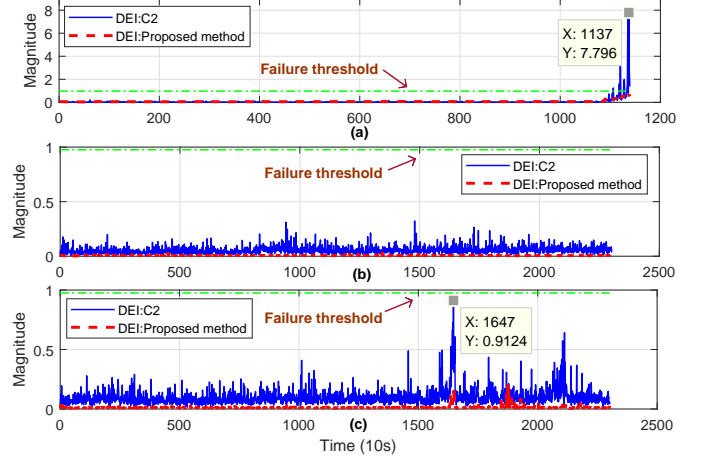


Figure 9. The comparison of the estimated DEIs extracted using HHT (DEI:C2) and calculated by trained CNN model (DEI:Proposed method) of (a) test bearing1_4, (b) test bearing1_5, and (c) test bearing1_6. Green dotted lines are the failure threshold.

To demonstrate the generality of our proposed RUL estimation framework, bearing2 operates under different external load and rotational speed are analyzed. Bearing2_2 is used for training, and the final trained CNN model is obtained without changing any hyper-parameters and architecture of those values in Table III. We just fine-tune the ϵ -SVR forecasting model by changing penalty parameter C from 5.09 to 7.09, resulting in 5.75% and 1.55% E_r for Bearing2_4 and bearing2_6, respectively. Good RUL prediction results of bearings with different operating conditions indicate the repeatability and robustness of our proposed method, with respect to the hyper parameters of the CNN as well as the architecture of the CNN.

To further verify the proposed approach, the predicted numerical errors of RULs generated by the proposed method and other published methods are listed and compared in Table VI. The other published approaches include a recurrent neural network method based health indicator [27], the method proposed by the winner of the IEEE PHM 2012 prognostic [38], and a convolutional long-short-term memory network method [39], etc.. The results of the comparison shown in Table VI confirm that our approach significantly outperforms the referenced methods with an average 3% E_r (average of absolute errors). In particular, a -0.29% E_r of bearing1_4 is achieved, owing to a 1s absolute time error. This result benefits from a good nonlinear degradation indicator extracted using the HHT method. This is different from other approaches shown in Table VI, where the linear time label is usually chosen as the degradation indicator for the underlying bearing

Table V
COMPARISON OF PREDICTED RESULTS BETWEEN PROPOSED APPROACH AND OTHER TESTED METHODS

Methods	Bearing1_4 ($T_{failure} = 339$ s)			Bearing1_5 ($T_{failure} = 1610$ s)			Bearing1_6 ($T_{failure} = 1460$ s)		
	$\bar{T}_{failure}$	$E_r\%$	ETA	$\bar{T}_{failure}$	$E_r\%$	ETA	$\bar{T}_{failure}$	$E_r\%$	ETA
Proposed approach	340 s	-0.29%	0.96	1500 s	6.83%	0.79	1480 s	-1.37%	0.83
C1	30 s	91.15%	0.04	820 s	49.07%	0.18	1181 s	19.11%	0.52
C2	N/A (0 s)	N/A (100%)	0.03	1140 s	29.19%	0.36	1080 s	26.02%	0.41

system, causing a less accurate prediction time. In addition, the CNN is a powerful tool for discovering the hidden pattern of the extracted degradation indicator and the underlying bearing system, further increasing the accuracy of the predicted RUL.

To sum up, it can be concluded from the experiment results that the proposed data-driven RUL estimation approach has much better prediction accuracy, compared with both the tested methods in this work and the other published methods in previous studies.

IV. CONCLUSION

In this paper, a new on-line data-driven framework for RUL of rolling element bearings is presented using HHT, a CNN model and an ϵ -SVR forecasting model. An experimentation platform that allows to observe the accelerated degradation process of bearings is employed to validate the proposed framework. A DEI is successfully extracted from the raw vibration signals, which is used as the label for the training of the CNN model. A CNN model is trained based on the extracted DEI and the raw vibration data of the training bearing. Predicted DEIs are automatically obtained when applying the CNN model to the test bearings. Finally, the RULs of the testing bearings are acquired using an ϵ -SVR forecasting model. The proposed framework achieves much higher accuracy for RUL estimation than previous published approaches.

Future work should mainly include the following: 1) the application of the proposed framework to a wider range of case studies on experimental data, and 2) the investigation of other potential degradation labels to achieve even higher accuracy in estimating RUL.

REFERENCES

- [1] T. A. Harris, *Rolling bearing analysis*. John Wiley and sons, 2001.
- [2] Y. Yuan, H.-T. Zhang, Y. Wu, T. Zhu, and H. Ding, "Bayesian learning-based model-predictive vibration control for thin-walled workpiece machining processes," *IEEE/ASME Transactions on Mechatronics*, vol. 22, no. 1, pp. 509–520, 2017.
- [3] H.-T. Zhang, B. Hu, L. Li, Z. Chen, X. Huang, G. Gu, and Y. Yuan, "Distributed hammerstein modeling for cross-coupling effect of multi-axis piezoelectric micropositioning stages," *Accepted. IEEE/ASME Transactions on Mechatronics*, 2018.
- [4] A. Heng, S. Zhang, A. C. Tan, and J. Mathew, "Rotating machinery prognostics: State of the art, challenges and opportunities," *Mechanical Systems and Signal Processing*, vol. 23, no. 3, pp. 724–739, 2009.
- [5] L. R. Rodrigues, "Remaining useful life prediction for multiple-component systems based on a system-level performance indicator," *IEEE/ASME Transactions on Mechatronics*, vol. 23, no. 1, pp. 141–150, 2018.
- [6] M. Pecht, *Prognostics and health management of electronics*. Wiley Online Library, 2008.
- [7] I. V. de Bessa, R. M. Palhares, M. F. S. V. D'Angelo, and J. E. Chaves Filho, "Data-driven fault detection and isolation scheme for a wind turbine benchmark," *Renewable Energy*, vol. 87, pp. 634–645, 2016.
- [8] J. Sikorska, M. Hodkiewicz, and L. Ma, "Prognostic modelling options for remaining useful life estimation by industry," *Mechanical Systems and Signal Processing*, vol. 25, no. 5, pp. 1803–1836, 2011.
- [9] Z.-Q. Wang, C.-H. Hu, and H.-D. Fan, "Real-time remaining useful life prediction for a nonlinear degrading system in service: Application to bearing data," *IEEE/ASME Transactions on Mechatronics*, vol. 23, no. 1, pp. 211–222, 2018.
- [10] Y. Li, T. Kurfess, and S. Liang, "Stochastic prognostics for rolling element bearings," *Mechanical Systems and Signal Processing*, vol. 14, no. 5, pp. 747–762, 2000.
- [11] X.-S. Si, W. Wang, C.-H. Hu, and D.-H. Zhou, "Remaining useful life estimation—a review on the statistical data driven approaches," *European Journal of Operational Research*, vol. 213, no. 1, pp. 1–14, 2011.
- [12] Z. Feng, M. Liang, and F. Chu, "Recent advances in time–frequency analysis methods for machinery fault diagnosis: A review with application examples," *Mechanical Systems and Signal Processing*, vol. 38, no. 1, pp. 165–205, 2013.
- [13] H. Gao, L. Liang, X. Chen, and G. Xu, "Feature extraction and recognition for rolling element bearing fault utilizing short-time fourier transform and non-negative matrix factorization," *Chinese Journal of Mechanical Engineering*, vol. 28, no. 1, pp. 96–105, 2015.
- [14] R. Yan, R. X. Gao, and X. Chen, "Wavelets for fault diagnosis of rotary machines: A review with applications," *Signal Processing*, vol. 96, pp. 1–15, 2014.
- [15] Q. Meng and L. Qu, "Rotating machinery fault diagnosis using wigner distribution," *Mechanical Systems and Signal Processing*, vol. 5, no. 3, pp. 155–166, 1991.
- [16] A. Soualhi, K. Medjaher, and N. Zerhouni, "Bearing health monitoring based on hilbert–huang transform, support vector machine, and regression," *IEEE Transactions on Instrumentation and Measurement*, vol. 64, no. 1, pp. 52–62, 2015.
- [17] Z. Peng, W. T. Peter, and F. Chu, "A comparison study of improved hilbert–huang transform and wavelet transform: application to fault diagnosis for rolling bearing," *Mechanical Systems and Signal Processing*, vol. 19, no. 5, pp. 974–988, 2005.
- [18] H. Li, Y. Zhang, and H. Zheng, "Hilbert–huang transform and marginal spectrum for detection and diagnosis of localized defects in roller bearings," *Journal of Mechanical Science and Technology*, vol. 23, no. 2, pp. 291–301, 2009.
- [19] J. Wu, C. Wu, S. Cao, S. W. Or, C. Deng, and X. Shao, "Degradation data-driven time-to-failure prognostics approach for rolling element bearings in electrical machines," *IEEE Transactions on Industrial Electronics*, 2018.
- [20] G. Cheng, Y.-L. Cheng, L.-h. Shen, J.-b. Qiu, and S. Zhang, "Gear fault identification based on hilbert–huang transform and som neural network," *Measurement*, vol. 46, no. 3, pp. 1137–1146, 2013.
- [21] Z. Tian, "An artificial neural network method for remaining useful life prediction of equipment subject to condition monitoring," *Journal of Intelligent Manufacturing*, vol. 23, no. 2, pp. 227–237, 2012.
- [22] W. Wang, "An adaptive predictor for dynamic system forecasting," *Mechanical Systems and Signal Processing*, vol. 21, no. 2, pp. 809–823, 2007.
- [23] X.-S. Si, W. Wang, C.-H. Hu, M.-Y. Chen, and D.-H. Zhou, "A wiener-process-based degradation model with a recursive filter algorithm for remaining useful life estimation," *Mechanical Systems and Signal Processing*, vol. 35, no. 1-2, pp. 219–237, 2013.
- [24] R. Huang, L. Xi, X. Li, C. R. Liu, H. Qiu, and J. Lee, "Residual life predictions for ball bearings based on self-organizing map and back propagation neural network methods," *Mechanical Systems and Signal Processing*, vol. 21, no. 1, pp. 193–207, 2007.

Table VI
COMPARISON OF PREDICTED RESULTS BETWEEN PROPOSED APPROACH AND EXISTING MAJOR APPROACHES

Methods	$E_r \%$				
	Bearing 1_4	Bearing 1_5	Bearing 1_6	Bearing 2_4	Bearing 2_6
Proposed approach	-0.29%	7.45%	-1.37%	5.75%	1.55%
RNN [27]	67.55%	-22.98%	21.23%	-19.42%	-13.95%
Particle Filtering [40]	5.60%	100.00%	28.08%	8.63%	58.91%
FFT+Ratio [38]	80.00%	9.00%	-5.00%	10%	49%
LSTM [39]	38.69%	-99.40%	-120.07%	19.81%	17.87%
Self-organization Mapping (SOM) [41]	-20.94%	-278.26%	19.18%	51.80%	-20.93%

- [25] Q. Wang, J. Gao, and Y. Yuan, “A joint convolutional neural networks and context transfer for street scenes labeling,” *IEEE Transactions on Intelligent Transportation Systems*, 2017.
- [26] C. Farabet, C. Couprie, L. Najman, and Y. LeCun, “Learning hierarchical features for scene labeling,” *IEEE Transactions on Pattern Analysis and Machine Intelligence*, vol. 35, no. 8, pp. 1915–1929, 2013.
- [27] L. Guo, N. Li, F. Jia, Y. Lei, and J. Lin, “A recurrent neural network based health indicator for remaining useful life prediction of bearings,” *Neurocomputing*, vol. 240, pp. 98–109, 2017.
- [28] Y. Yuan, C. Tian, and X. Lu, “Auxiliary loss multimodal gru model in audio-visual speech recognition,” *IEEE Access*, vol. 6, pp. 5573–5583, 2018.
- [29] G. Hinton, L. Deng, D. Yu, G. E. Dahl, A.-r. Mohamed, N. Jaitly, A. Senior, V. Vanhoucke, P. Nguyen, T. N. Sainath *et al.*, “Deep neural networks for acoustic modeling in speech recognition: The shared views of four research groups,” *IEEE Signal Processing Magazine*, vol. 29, no. 6, pp. 82–97, 2012.
- [30] M. Baptista, E. M. Henriques, I. P. de Medeiros, J. P. Malere, C. L. Nascimento Jr, and H. Prendinger, “Remaining useful life estimation in aeronautics: Combining data-driven and kalman filtering,” *Reliability Engineering & System Safety*, 2018.
- [31] Y. Lei, N. Li, L. Guo, N. Li, T. Yan, and J. Lin, “Machinery health prognostics: A systematic review from data acquisition to rul prediction,” *Mechanical Systems and Signal Processing*, vol. 104, pp. 799–834, 2018.
- [32] N. Tandon and A. Choudhury, “A review of vibration and acoustic measurement methods for the detection of defects in rolling element bearings,” *Tribology International*, vol. 32, no. 8, pp. 469–480, 1999.
- [33] Y. LeCun, Y. Bengio, and G. Hinton, “Deep learning,” *Nature*, vol. 521, no. 7553, p. 436, 2015.
- [34] Y.-L. Boureau, J. Ponce, and Y. LeCun, “A theoretical analysis of feature pooling in visual recognition,” in *Proceedings of the 27th International Conference on Machine Learning (ICML-10)*, 2010, pp. 111–118.
- [35] D. P. Kingma and J. Ba, “Adam: A method for stochastic optimization,” *arXiv preprint arXiv:1412.6980*, 2014.
- [36] T. Benkedjouh, K. Medjaher, N. Zerhouni, and S. Rechak, “Remaining useful life estimation based on nonlinear feature reduction and support vector regression,” *Engineering Applications of Artificial Intelligence*, vol. 26, no. 7, pp. 1751–1760, 2013.
- [37] P. Nectoux, R. Gouriveau, K. Medjaher, E. Ramasso, B. Chebel-Morello, N. Zerhouni, and C. Varnier, “Pronostia: An experimental platform for bearings accelerated degradation tests,” in *IEEE International Conference on Prognostics and Health Management, PHM’12*. IEEE Catalog Number: CPF12PHM-CDR, 2012, pp. 1–8.
- [38] E. Sutrisno, H. Oh, A. S. S. Vasan, and M. Pecht, “Estimation of remaining useful life of ball bearings using data driven methodologies,” in *Prognostics and Health Management (PHM), 2012 IEEE Conference on*. IEEE, 2012, pp. 1–7.
- [39] A. Z. Hinchi and M. Tkiouat, “Rolling element bearing remaining useful life estimation based on a convolutional long-short-term memory network,” *Procedia Computer Science*, vol. 127, pp. 123–132, 2018.
- [40] Y. Lei, N. Li, S. Gontarz, J. Lin, S. Radkowski, and J. Dybala, “A model-based method for remaining useful life prediction of machinery,” *IEEE Transactions on Reliability*, vol. 65, no. 3, pp. 1314–1326, 2016.
- [41] S. Hong, Z. Zhou, E. Zio, and K. Hong, “Condition assessment for the performance degradation of bearing based on a combinatorial feature extraction method,” *Digital Signal Processing*, vol. 27, pp. 159–166, 2014.